AIP Journal of Applied Physics

Raman scattering of rare earth sesquioxide Ho2O3: A pressure and temperature dependent study

Sugandha Dogra Pandey, K. Samanta, Jasveer Singh, Nita Dilawar Sharma, and A. K. Bandyopadhyay

Citation: Journal of Applied Physics **116**, 133504 (2014); doi: 10.1063/1.4896832
View online: http://dx.doi.org/10.1063/1.4896832
View Table of Contents: http://scitation.aip.org/content/aip/journal/jap/116/13?ver=pdfcov
Published by the AIP Publishing

Raman scattering of rare earth sesquioxide Ho_2O_3: A pressure and temperature dependent study

Sugandha Dogra Pandey, K. Samanta, Jasveer Singh, Nita Dilawar Sharma, and A. K. Bandyopadhyay
Pressure & Vacuum Standards, National Physical Laboratory, Dr. K.S. Krishnan Road, New Delhi 110012, India

(Received 23 June 2014; accepted 19 September 2014; published online 1 October 2014)

Pressure and temperature dependent Raman scattering studies on Ho_2O_3 have been carried out to investigate the structural transition and the anharmonic behavior of the phonons. Ho_2O_3 undergoes a transition from cubic to monoclinic phase above 15.5 GPa, which is partially reversible on decompression. The anharmonic behavior of the phonon modes of Ho_2O_3 from 80 K to 440 K has been investigated. We find an anomalous line-width change with temperature. The mode Grüneisen parameter of bulk Ho_2O_3 was estimated from high pressure Raman investigation up to 29 GPa. Furthermore, the anharmonic components were calculated from the temperature dependent Raman scattering. © *2014 AIP Publishing LLC*. [http://dx.doi.org/10.1063/1.4896832]

I. INTRODUCTION

Rare earth oxides with unique electronic properties are the potential candidates for applications such as catalysts, high dielectric constant gate oxides, dopants for lasers, and materials for magneto-optic memory.[1] Among these, the rare earth sesquioxide Ho_2O_3 is highly insoluble in water and a thermally stable holmium source suitable for glass, optic, and ceramic applications. It is used in producing metal halide lamps, and is also used as an additive of various garnets. Similar to most other oxides of rare-earth elements, holmium oxide is used as a speciality catalyst, phosphor and a laser material. Holmium oxide occurs in small quantities in the minerals monazite, gadolinite, and in other rare-earth minerals.[2] Ho_2O_3 occurs naturally as C-type rare earth oxide, which crystallizes in the space group *Ia*-3 (No. 206) with elementary cell containing 16 formula units RE_2O_3. The 32 cations are distributed among two different sites: 24 in d sites with local symmetry C_2 (2) (non-centro-symmetric), and 8 in b sites with local symmetry C_{3j} (3 m, or S6) (centro-symmetric). The 48 oxygen ions in the body-centered cell are on general positions 48e with C_1 site symmetry.[3] The electronic configuration of the Ho ion in Ho_2O_3 is [Xe] $4f^{11}$ $5s^2$ $5p^6$. The ten f-electrons are localized in the 4*f* shell with one *f*-electron in the conduction band making Ho trivalent. However, Ho_2O_3 along with other rare earth sesquioxides also occurs in other structural/polymorphic modifications, which include monoclinic with space group C_2/m and hexagonal with space group P3m1.

To address the issues of stability and structural transformations, metal-insulator transitions, enhancement or collapse of magnetic ordering and amorphization, etc., high pressure investigations play a pivotal role. Under such conditions, the bonding patterns established for the systems near ambient conditions change dramatically, causing profound effects on numerous physical and chemical properties and leading to the formation of new classes of materials. Although a number of rare earth sesquioxides have been investigated under pressure,[4–9] the structural stability of Ho_2O_3 has received much less attention.[6,9]

Further, the Raman spectra of phonons have a very high sensitivity, which permits finger-printing analysis of composition and state of a material. Hence Raman scattering is one of the most powerful techniques to investigate the phonon spectrum, electron phonon coupling, structural phase transitions, and anharmonic behavior of the optical modes. The high pressure Raman studies in conjunction with temperature dependent behavior reveal the phonon-phonon couplings and their effect on the structure and stability. To the best of our knowledge, there are no reports of observance of a clear phase transition in the Raman spectra of Ho_2O_3. Although Lonappan *et al.*[6] demonstrated a clear phase transition using X-ray diffraction, their Raman data did not depict a clear transition.

With change in temperature, most materials typically show both the line centre and the line-width variation in their Raman spectra. This temperature dependence can be attributed to the anharmonic terms in the vibrational potential energy. Size effects in nanocrystals are also expected to modify the anharmonicity and the phonon decay times as compared to their bulk/polycrystalline counterparts. Again, the anharmonic parameters for Ho_2O_3 have not been investigated earlier, to the best of our knowledge. The estimation of these anharmonic parameters requires the mode Grüneisen parameter, which is obtained from the pressure dependent frequency variation of the phonon modes. Hence in this report, we also present the estimation of anharmonic parameters using data from our own high pressure experiment.

II. EXPERIMENTAL

Commercially available Ho_2O_3 powder from Johnson Matthey Inc, UK, was used for the present study and no pretreatment was done. The X-ray diffractogram of the powder was recorded using Bruker D-8 Advance powder X-Ray diffractometer using Cu k_α ($\lambda = 1.5404$ Å) radiation. The high-pressure Raman scattering studies were carried out with a

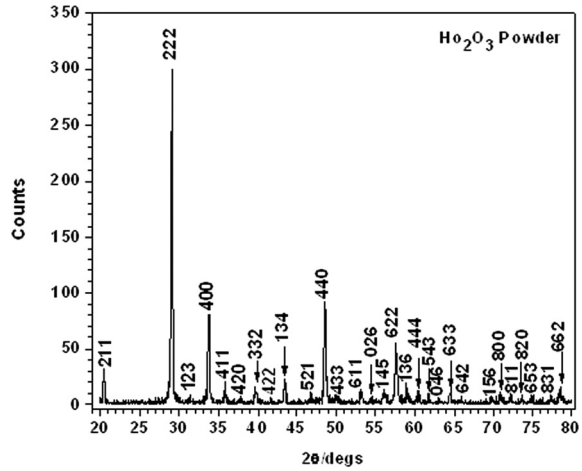

FIG. 1. X-ray diffraction pattern for the Ho_2O_3 sample under study.

single stage Jobin-Yvon Spex monochromator using an Ar^+ ($\lambda = 514.5$ nm) ion laser. The Raman signal was detected by a liquid nitrogen cooled charge couple device (CCD). A Mao-Bell type diamond anvil cell (DAC) with octagonal flats having about 400 μm diameter culets was used to generate high pressure up to 28 GPa. The sample was loaded in the drilled gasket hole along with a few small ruby chips (5–10 μm) for monitoring the pressure in Raman experiments. The pressure transmitting medium used was methanol: ethanol in the ratio of 4:1. The temperature dependent Raman measurements were performed in the backscattering geometry using the Jobin-Yvon T64000 Triple-mate instrument coupled with the Ar^+ 514.5 nm laser line. A charge-coupled device system with an accuracy of ($0.75\,cm^{-1}$) was used to collect the scattered data. The sample temperature was varied from 80–440 K by using a continuous flow liquid nitrogen optical cryostat in which the sample compartment was maintained at a pressure of $\sim 10^{-6}$ torr using a turbo-molecular pump.

III. CHARACTERIZATION AT AMBIENT

Figure 1 shows the x-ray diffraction pattern of Ho_2O_3 powder, which agrees with the JCPDS data card number 43–1018 for cubic (Ia_3) Ho_2O_3 structure. The coherent crystalline size was estimated using Scherrer equation,[10] using the diffraction from the [222] plane of cubic Ho_2O_3. After accounting for the instrument broadening, the average crystallite size was estimated to be $\sim$50 nm.[10]

Further particle size analysis was carried out using AFM and Figures 2(a) and 2(b) show the atomic force micrographs of Ho_2O_3. The "Image Tool" software was used to estimate the distribution in particle size. Figure 2(c) shows the histogram for the same. Consequently, the average particle size was calculated to be around 63 nm. The difference obtained in the sizes obtained from XRD and AFM studies may arise due to cluster effects in AFM. However, from both the studies, it is apparent that the sample under study is nanocrystalline holmium sesquioxide.

In the cubic phase of Ho_2O_3, there are thirty two (32) Ho cations, which are distributed in two different sites, eight atoms are in C_{3i} site symmetry with coordinate (¼ ¼ ¼); and twenty four atoms are in C_2 site symmetry with coordinate (x 0 ¼). The forty eight oxygen atoms in bcc structure are positioned at C_1 site symmetry.[3,8] The local axes of the C_{3i} sites are in the

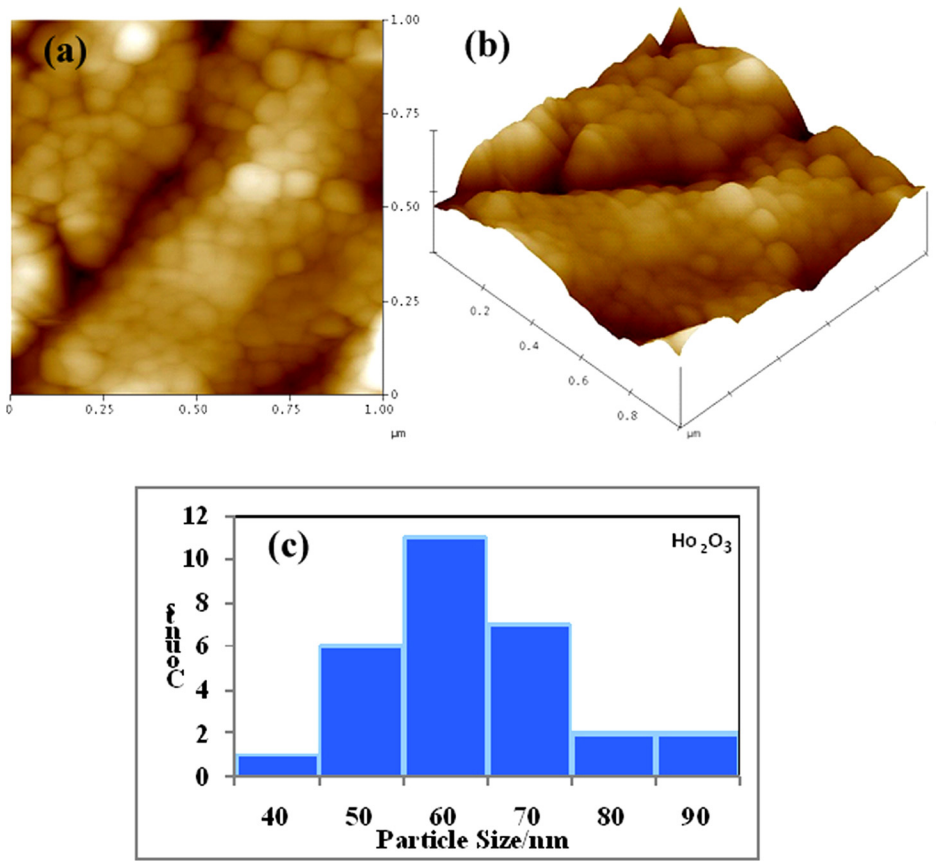

FIG. 2. Atomic force micrographs (a) 2d view (b) 3d view, (c) particle size distribution deduced using the "image tool" software.

[111], [$\bar{1}$11], [1$\bar{1}$1], and [11$\bar{1}$] directions; whereas the C_2 axes are parallel to [100], [010], or [001] directions. According to group theory, the irreducible representations of vibrations of atoms occupying the sites give 22 Raman active optical modes of cubic Ho_2O_3, which include $4A_g$, $4E_g$, and $14T_g$ modes. However, smaller numbers of modes are observed in practice in the Raman spectra; this may be due to the fact that some of the observed modes are actually superposition of closely spaced different type of modes, which are un-separated owing to a weak factor-group interaction.[11]

The Raman spectra of Ho_2O_3 powder at 80 and 300 K are shown in Fig. 3. The peaks obtained under ambient conditions agree very well with the results published by Urban and Cornilson.[12] We have observed seven distinct peaks (I_1–I_7) at 80 K; the peaks at 317.3, 332, 361.5, 379.4, 439.2, 473.6, and 595.3 cm^{-1} are assigned as the $T_g + E_g$, E_g, Γ_{el} (C_{3i}), $T_g + A_g$, and $3T_g$ modes, respectively.[11–15] The peak at 379.4 cm^{-1}, corresponding to the $T_g + A_g$ mode, is the most intense and would primarily be tracked for pressure as well as temperature dependent variations.

We have observed the electronic contribution Γ_{el} at 361.5 cm^{-1}. In *C*-type Ho_2O_3, the Ho^{3+} ions in C_{3i} sites have electronic configuration [(Xe) $4f^{10}$)], the crystal-field and spin-orbit interaction splits the unfilled *f*-orbital into the multiplates. The observed 361.5 cm^{-1} peak in the Raman spectrum is the electronic transition originated from stark energy level $^5I_8$ of Ho^{3+} in Ho_2O_3.[16] The electronic contribution reduced significantly at 300 K, as shown in the inset of Fig. 3. In addition, it may be suspected that a slight amount of disordered material may also be present owing to the broad backgrounds in the Raman spectra. Further, the significantly increased background in the Raman spectrum at 80 K is expected to originate from the intra-band radiative recombination of electron in Ho_2O_3, whose intensity decreases with increasing temperature.

IV. HIGH PRESSURE BEHAVIOR

The pressure dependent Raman spectra of this nanocrystalline Ho_2O_3 powder are shown in Fig. 4(a). It is clear that the intensity of the modes related to cubic phase at ambient decrease significantly and the mode frequencies shift towards higher energy side with increasing pressure. At a pressure of about 1.3 GPa, new peaks are seen to be emerging between 600 and 700 cm^{-1} and their intensity increases with the progression in applied pressure; while the peaks related to the cubic phase gradually broaden with an intensity decrease. At a pressure of about 17.8 GPa, the predominant cubic phase peak completely disappears. However, the peaks observed between 600–700 cm^{-1} are seen to gain intensity from pressures as low as 5.5 GPa. In fact at the highest studied pressure of about 28.8 GPa, most other peaks disappear and the peaks which remain are centered at 697, 751, 822, and 947 cm^{-1}, with another weaker band at 1084 cm^{-1}. Hence the cubic phase is seen to completely transform to a new structural phase above 15.5 GPa and the transition is completed at 17.8 GPa. These new peaks, and the phase, have been identified as occurring due to the development of the monoclinic phase and compare well with the reported peaks for monoclinic Ho_2O_3.[3] Also, in analogy with the monoclinic spectra of other rare earth sesquioxides,[17–21] the developed phase has been confirmed as the monoclinic phase. Heiba *et al.*[3] have also reported similar development of monoclinic phase related Raman peaks of Ho_2O_3 in their $Dy_{2-x}Ho_xO_3$ samples for $x \geq 0.4$. Similar behavior of Raman peaks in Lu_2O_3 under pressure has been reported by

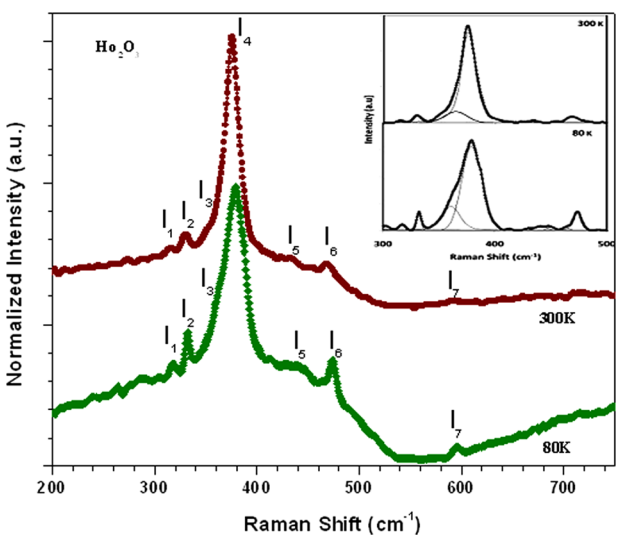

FIG. 3. Phonon spectra of Ho_2O_3 sample at 80 and 300 K. Inset shows the de-convoluted peaks for better visualization.

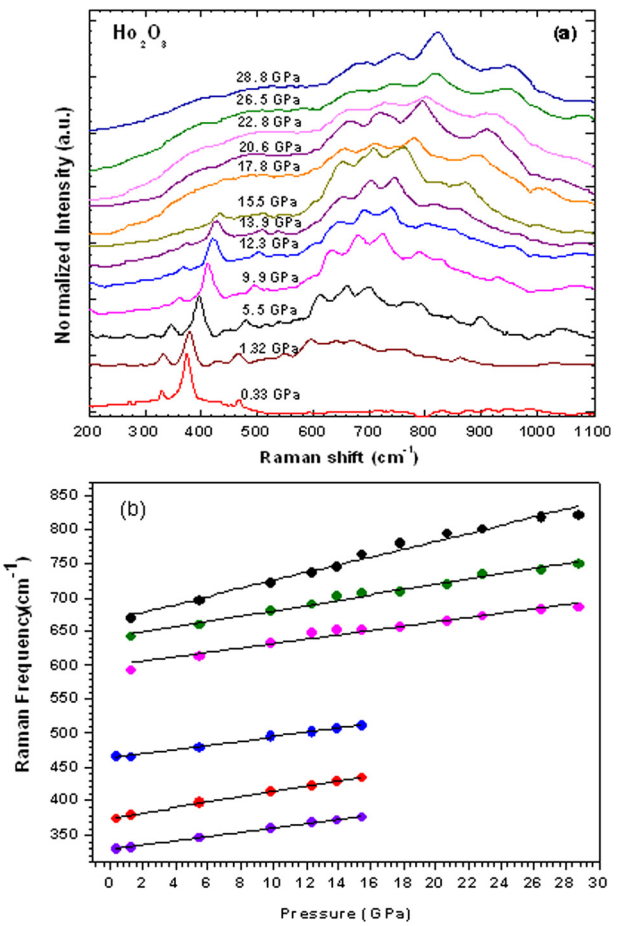

FIG. 4. (a) Raman spectra for Ho_2O_3 as a function of increasing pressures; (b) Raman frequency shifts of Ho_2O_3 phonon modes as function of pressure.

Jiang *et al.*[9] The peak at 1084 cm^{-1} at 28.8 GPa may be the result of crystal field excitation.[9] Hence, we may surmise that in case of Ho_2O_3, the phase transition to monoclinic structure completes at 17.8 GPa with complete disappearance of the predominating cubic phase peak. Figure 4(b) shows the pressure dependent frequency shifts.

The monoclinic B-type structure of lanthanide sesquioxides belongs to the centro-symmetric space group C_2/m (C_{2h}^3), which contains six molecules in each unit cell, and also shows a sevenfold coordination of the cation. The crystal lattice has three different cation sites and five different anion sites which bond to four, five, or six metal ions.[20,22] In B-type structure, Ho atoms are located in three different 4*i* positions. The 18 oxygen atoms of the unit cell occupy five different crystallographic sites: four in 4*i* (m or C_s symmetry) = O (1), O (2), O (3), O (4), i.e., 16 O in *4i*; one in *2b* (2/*m* or C_{2h} symmetry) = O (5), i.e., 2 O in 2b.[16,20,22] Hence, the irreducible representation according to group theory gives 21 Raman active modes which include $14A_g$ and $7B_g$ modes. Gouteron *et al.*[17] also predicted 21 Raman active modes, i.e., $14A_g + 7B_g$, from the factor group analysis for B-type crystals, although fewer modes are observed in practice. We have calculated the mode Grüneisen Parameter (γ), which provides a dimensionless representation of the response to compression from the pressure dependent frequency shifts $d\omega/dP$ (Fig. 4(b)), i.e.,

$$\omega = \omega_0 + (d\omega/dP)P. \quad (1)$$

The mode Grüneisen parameters are obtained from the equation:[23]

$$\gamma_i = (B_0/\omega_0)(d\omega/dP), \quad (2)$$

where B_0 is the isothermal bulk modulus of Ho_2O_3 of the cubic phase, ω_0 is the mode frequency at ambient. The isothermal bulk modulus values of Ho_2O_3 were taken as 206 and 200 GPa for the cubic and monoclinic phase, respectively.[9] The obtained γ values are tabulated in Table I. These values for Ho_2O_3 have not been reported so far to the best of our knowledge. The monoclinic modes obtained after extrapolation of the high pressure peaks to the atmospheric pressure are also presented in Table I.

Figure 5 shows the behavior of the sample on decompression. The peaks occurring due to monoclinic phase shift to lower wave numbers with decompression. However, the sample shows partial reversible behavior although the high pressure phase is observed down to the ambient. Broad peaks around 415 and 460 cm^{-1} are seen to be developing as decompression progresses, which qualitatively depict the partial reversibility of the observed transition.

TABLE I. The mode frequencies, pressure coefficients, and Grüneisen parameters (γ_i) for phonon modes in cubic Ho_2O_3.

Phase/structure	$\omega(cm^{-1})$	$d\omega/dp(cm^{-1}/GPa)$	γ_i
Cubic	330.2	3.19	1.99
	375.2	3.89	2.14
	468	3.05	1.34
Monoclinic	608	3.24	1.07
	652.3	3.84	1.18
	682.7	5.74	1.68
	760	7.9	2.08

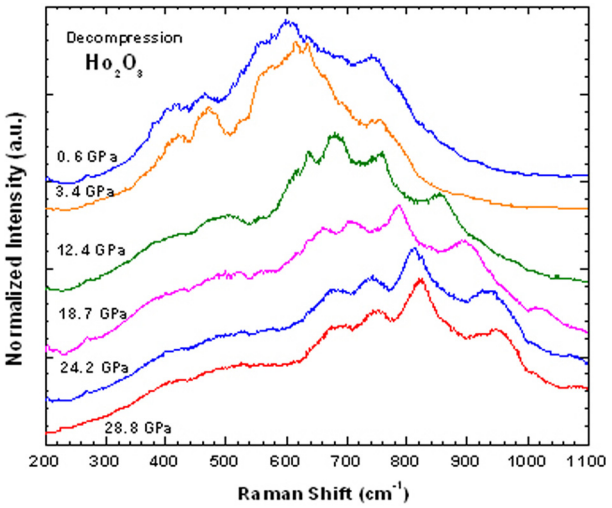

FIG. 5. Raman spectra of Ho_2O_3 observed during the releasing pressure cycle.

A. Discussion

In the present study, it is interesting to note that contrary to the cubic to hexagonal phase transitions observed in our previous reports of Dy_2O_3 and Yb_2O_3,[24,25] Ho_2O_3 shows a different response to the applied pressure and converts to the monoclinic phase. However, this behavior has been found to be similar to our previous studies on Sm_2O_3 and Eu_2O_3.[24,26] It is noteworthy that there exist several ways of transformation between the various phases, depending on temperature and pressure conditions.[27,28] Additional reaction components can also help to transform the sesquioxides during the temperature treatment. For example, Foex *et al.* achieved a transformation from the C-type to the B-type structure by adding some lime,[29] or by offering support with oxides like CaO and SrO.[30] In the previous similar observations in the case of Eu_2O_3 and Sm_2O_3, the starting material was found to contain traces of non-stoichiometric phase and monoclinic phase, respectively.[24,26] In the present case also at ambient and at a low pressure of 1.32 GPa, a broad hump is seen around 600–700 cm^{-1}, which increases with applied pressure. Although our XRD studies did not indicate the presence of another phase, it may be possible that some amount of disordered state is present in the sample, which facilitates the growth of monoclinic phase at the expense of cubic phase.

In context of the reported work, it has been observed that the structural stability of Ho_2O_3 under high pressure has received much less attention as compared to other rare earth sesquioxides. Based on the density functional theory calculations, Wu *et al.*[31] predicted a B→A phase transition in Ho_2O_3 at around 17.0 GPa. The C-type Ho_2O_3 has also been reported to transform to the monoclinic phase at 1.5 GPa and 1000 °C by Hoekstra.[32] Lonappan *et al.* carried out the study on cubic Ho_2O_3 up to 17.0 GPa by using rotating anode x-ray generator and reported that a phase transformation of

C→B appeared between 9.5 and 16.0 GPa,[6] but the B→A phase transition was not observed. Recently, Jiang *et al.*,[9] using x-ray diffraction, also observed the structural transformation from a cubic to a monoclinic structure starting at 8.9 GPa, which completed at 16.3 GPa with a 8.1% volume collapse. A hexagonal phase appeared at 14.8 GPa and becomes dominant at 26.4 GPa. After release of pressure, the hexagonal phase transformed to a monoclinic structure. However, the observance of a clear phase transition in Raman spectra of Ho_2O_3 is not reported so far. Hence qualitatively, our results also agree somewhat with the pressures reported for the completion of phase transformation.

The structural characterization of monoclinic (B) Ho_2O_3, synthesized by Hoekstra, has been reported by a few workers.[32,33] It was figured out that the phase transformations of the cubic rare-earth sesquioxides into the monoclinic compounds (C–B transformation) are reversible under certain high-pressure/high-temperature conditions between 2.5 and 4 GPa at 900–1000 °C.[32] Sawyer *et al.* succeeded in transforming parts (~20%) of the cubic phase starting material C-Ho_2O_3 by high-pressure impact methods.[34] Hoekstra[33] and Sawyer[34] showed that the monoclinic phase B-Ho_2O_3 disappears under temperature treatment and is transformed into the cubic phase C-Ho_2O_3, which supported the prediction of a metastable high-pressure phase.[33]

V. TEMPERATURE DEPENDENT BEHAVIOR

The anharmonic behavior of the phonon modes has been investigated by the temperature dependent Raman scattering in the range of 80–440 K. The temperature dependent Raman spectra of Ho_2O_3 are shown in Fig. 6(a). The most intense $T_g + A_g$ mode is seen to be shifting towards lower frequency side with increasing temperature; however, other modes do not change significantly. The variation/shift in frequency of $T_g + A_g$ mode is plotted in Fig. 6(b). This shift of frequency with temperature has contribution from the thermal expansion of the lattice and anharmonic phonon-phonon interaction. The phonon frequency shift as a function of temperature can be expressed as,[34,35]

$$\omega(T) = \omega_0 + (\Delta\omega)_{latt} + (\Delta\omega)_{anh}, \tag{3}$$

where ω_0 is harmonic frequency, which was obtained by extrapolating the experimental data down to 0 K; the quasi harmonic term $(\Delta\omega)_{latt}$ arises from the thermal expansion while $(\Delta\omega)_{anh}$ represents the anharmonic coupling of the phonons.

The quasi-harmonic or thermal expansion contribution can be written as[36]

$$(\Delta\omega)_{latt} = \omega_0\left\{\exp\left[-\gamma_i\int_0^T 3\alpha(T)dT\right] - 1\right\}, \tag{4}$$

where ω_0 is the harmonic frequency of $T_g + A_g$ mode. The Grüneisen parameter of the corresponding mode $\gamma_i = 2.14$ is estimated from our high pressure Raman scattering data. The linear thermal expansion coefficient, $\alpha = 7.4 \times 10^{-6}$/K for Ho_2O_3.[37]

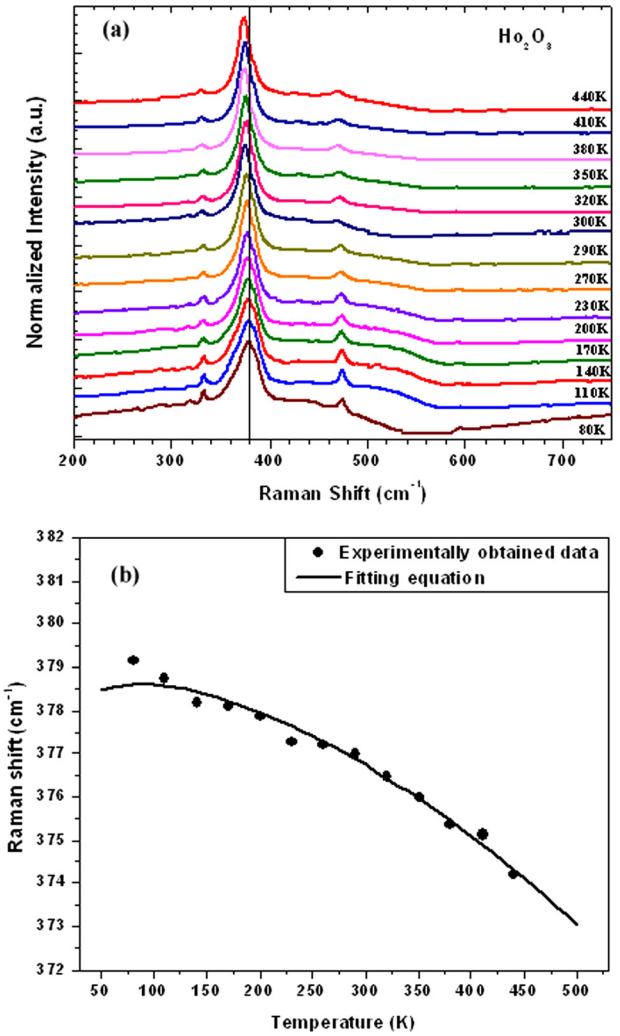

FIG. 6. (a) Temperature dependent Raman spectra of Ho_2O_3 sample in the temperature range 80–440 K. (b) Shift of $T_g + A_g$ mode as a function of temperature, the solid line represents the fitting of the experimental data points using Eq. (3).

The anharmonic contribution $(\Delta\omega)_{anh}$ which arises from the phonon-phonon interaction due to the cubic and quartic terms in the inter-atomic potential, can be written as:[36]

$$(\Delta\omega)_{anh} = A\left[1 + \frac{2}{\exp(\hbar\omega_0/2kT) - 1}\right] + B\left[1 + \frac{3}{\exp(\hbar\omega_0/3kT) - 1} + \frac{3}{(\exp(\hbar\omega_0/3kT) - 1)^2}\right]. \tag{5}$$

The first term estimates the coupling of an optical phonon to two low-energy phonons (three phonon process); the second term is due to the coupling to three phonons (four-phonon process), while A and B are the fitting parameters. Equations (4) and (5) substituted into Eq. (3) give us the fitting expression. The experimental data are in good agreement with the fitting by Eq. (3), and fitting parameters are listed in Table II.

We have also calculated the total anharmonicity of $T_g + A_g$ mode as a function of temperature using the following equation:[38,39]

TABLE II. Best-fit values for anharmonic constants, true and quasi-harmonic contributions in $T_g + A_g$ mode of Ho_2O_3.

ω_0 (cm^{-1})	Γ_0 (cm^{-1})	A (cm^{-1})	B (cm^{-1})	$\frac{d\omega}{dT}$ ($cm^{-1}K^{-1}$)	$\left(\frac{1}{\omega_i}\frac{d\omega_i}{dT}\right)_P$ (K^{-1})	$\left(\frac{1}{\omega_i}\frac{d\omega_i}{dT}\right)_V$ (K^{-1})	$\gamma_i\alpha$ (K^{-1})
380.2	24.51	−2.74	−0.24	−0.012	-3.183×10^{-5}	-1.603×10^{-5}	1.58×10^{-5}

$$\left(\frac{1}{\omega_i}\frac{d\omega_i}{dT}\right)_P = \left(\frac{1}{\omega_i}\frac{d\omega_i}{dT}\right)_V - \gamma_i\alpha. \quad (6)$$

The first term of right hand side describe the true anharmonic contribution and second, quasi-harmonic term. The calculated values are listed in Table II. From the table, it is clear that the coefficients A and B both are negative, thus explaining the phonon softening. The three phonon process dominates over the quatric anharmonicity. It is also observed that the true anharmonic term is comparable to the quasi-harmonic term.

The temperature dependent line-width of the $T_g + A_g$ mode (Fig. 7) shows an anomalous behavior, demonstrating a decrease in line-width with an increase in temperature. In an ideal crystal, the line-shape is expected to be infinitesimally narrow, but experimental peaks of real materials exhibit an intrinsic width.[40] The line-width analysis of real materials is more difficult to achieve since different contributions have to be considered. Among these, the finite resolution of the spectrometer,[41] impurities and defects disturb the translation symmetry of the harmonic crystal.[40] All these factors along with the anharmonic decay of phonons account for the broadening observed. The thermal expansion is a manifestation of the lattice anharmonicity that has its own shifts in the frequency, but not on the line-width.[36] Hence, when other effects due to impurities, defects, and spectrometer are constants for a particular sample, the line-width variation would reflect the anharmonic decay of phonons. In the present case, the reason for an anomalous decrease in line-width is unclear, however, it may have contribution from the fact that owing to the presence of disordered material in the starting sample, the crystallinity improved with the increase of temperature with a decrease in the content of defects/disordered material. Consequently, the effect of anharmonic decay of phonons on the line-width variation cannot be precisely determined.

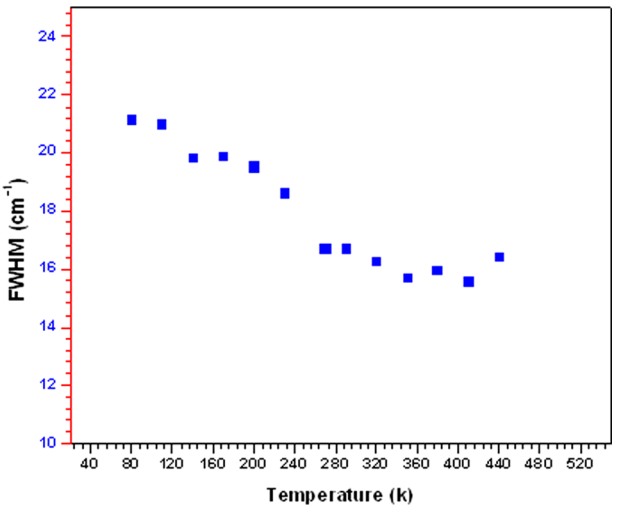

FIG. 7. FWHM of the $T_g + A_g$ mode as function of temperature T.

VI. CONCLUSIONS

We have investigated the behavior of phonon modes of rare earth Ho_2O_3 as a function of pressure and temperature. The high pressure Raman investigation reveals the cubic to monoclinic phase transition at and above 17.8 GPa, and this transition is partially reversible in nature. The mode Grüneisen parameters estimated from the high pressure data were used to estimate the anharmonicity components in conjunction with the temperature dependent shift behavior of the phonon modes in the range of 80–440 K. From the theoretical fitting to the experimental data, the cubic anharmonicity is observed to dominate over quatric anharmonicity. Further, the true anharmonic term is comparable to the quasi-harmonic or the thermal expansion term in determining the total anharmonicity. We found an anomalous behavior of phonon line width with increasing temperature.

ACKNOWLEDGMENTS

The authors wish to acknowledge the constant encouragement and support from Director, NPL. The authors are also grateful to CSIR for a research grant under NWP-45 network project.

[1]R. Gillen, S. J. Clark, and J. Robertson, Phys. Rev. B **87**, 125116 (2013).
[2]See http://www.americanelements.com/hoox.html for general information about Ho_2O_3, e.g., general properties, occurrence, structure etc., which are mentioned in the first paragraph of the introduction of our manuscript.
[3]Z. K. Heiba, M. B. Mohamed, and H. Fuess, Cryst. Res. Technol. **47**(5), 535–540 (2012).
[4]Q. X. Guo, Y. S. Zhao, C. Jiang, W. L. Mao, Z. W. Wang, J. Z. Zhang, and Y. J. Wang, Inorg. Chem. **46**, 6164 (2007).
[5]D. Liu, W. Lei, Y. Li, Y. Ma, J. Hao, X. Chen, Y. Jin, D. D. Liu, S. Yu, Q. L. Cui, and G. T. Zou, Inorg. Chem. **48**, 8251 (2009).
[6]D. Lonappan, N. V. Chandra Shekar, T. R. Ravindran, and P. C. Sahu, Mater. Chem. Phys. **120**, 65 (2010).
[7]E. Husson, C. Proust, P. Gillet, and J. P. Itié, Mater. Res. Bull. **34**, 2085 (1999).
[8]C. Meyer, J. P. Sanchez, J. Thomasson, and J. P. Itié, Phys. Rev. B **51**(18), 12187 (1995).
[9]S. Jiang, J. Liu, X. Li, L. Bai, W. X. Y. Zhang, C. Lin, Y. Li, and Li Tang, J. Appl. Phys. **110**, 013526 (2011).
[10]P. Scherrer, Göttinger Nachrichten Math. Phys. **2**, 98 (1918).
[11]G. Schaack and J. Koningstein, Opt. Soc. Am. **60**, 1110 (1970).
[12]M. W. Urban and B. C. Cornilsen, J. Phys. Chem. Solids **48**(5), 475 (1987).
[13]J. C. Panitz, J. C. Mayor, B. Grob, and W. Durisch, J. Alloys Compd. **303–304**, 340 (2000).
[14]N. Dilawar, S. Mehrotra, D. Varandani, B. V. Kumaraswamy, S. K. Haldar, and A. K. Bandyopadhyay, Mater. Charact. **59**, 462 (2008).
[15]W. B. White and V. G. Keramidas, Spectrochim. Acta A **28**, 501 (1972).
[16]C. Gheorghe, A. Lupei, V. Lupei, L. Gheorghe, and A. Ikesue, J. Appl. Phys. **105**, 123110 (2009).
[17]J. Gouteron, D. Michel, A. M. Lejus, and J. Zarembowitch, J. Solid State Chem. **38**, 288 (1981).
[18]C. L. Luyer, A. Garcia-Murillo, E. Bernstein, and J. Mugnier, J. Raman Spect. **34**, 234 (2003).

[19]F. X. Zhang, M. Lang, J. W. Wang, U. Becker, and R. C. Ewing, Phys. Rev. B. **78**, 064114 (2008).
[20]J. Zarembowitch, J. Gouteron, and A. M. Lejus, J. Raman Spectrosc. **9**(4), 263 (1980).
[21]L. Laversenne, Y. Guyot, C. Goutaudier, M. T. Cohen-Adad, and G Boulon, Opt. Mater. **16**, 475 (2001).
[22]S. A. Hering and H. Huppertz, Z. Naturforsch. **64**, 1032 (2009).
[23]G. K. Pradhan, A. Bera, P. Kumar, D. V. S. Muthu, and A. K. Sood, Solid State Commun. **152**(4), 284 (2012).
[24]N. Dilawar, D. Varandani, S. Mehrotra, H. Poswal, S. M. Sharma, and A. K. Bandyopadhyay, Nanotechnology **19**(11), 115703 (2008).
[25]S. Dogra Pandey, K. Samanta, J. Singh, N. Dilawar Sharma, and A. K. Bandyopadhyay, AIP Adv. **3**, 122123 (2013).
[26]N. Dilawar, D. Varandani, V. P. Pandey, M. Kumar, S. M. Shivaprasad, P. K. Sharma, and A. K. Bandyopadhyay, J. Nanosci. Nanotechnol. **6**, 105 (2006).
[27]M. Foex, Bull. Soc. Min. Crist. **88**, 521(1965).
[28]I. Warshaw and R. Roy, J. Phys. Chem. **65**(11), 2048 (1961).
[29]M. Foex and J. P. Traverse, Bull. Soc. Min. Crist. **89**, 184 (1966).
[30]M. Foex, Z. Anorg. Allg. Chem. **337**, 313 (1965).
[31]B. Wu, M. Zinkevich, F. Aldinger, D. Wen, and L. Chen, J. Solid State Chem. **180**(11), 3280 (2007).
[32]H. R. Hoeskstra, Inorg. Chem. **5**(5), 754 (1966).
[33]H. R. Hoekstra and K. Gingerich, Science **146**(3648), 1163 (1964).
[34]J. O. Sawyer, B. G. Hyde, and L. R. Eyring, Inorg. Chem. **4**, 426 (1965).
[35]Z. Dohcevic-Mitrovic, Z. V. Popovic, and M. Scepanovic, Acta Phys. Polonica A **116**(1), 36 (2009).
[36]K. Samanta, P. Bhattacharya, and R. S. Katiyar, Phys. Rev. B **75**, 035208 (2007).
[37]J. E. Spanier, R. D. Robinson, F. Zhang, S.-W. Chan, and I. P. Herman, Phys. Rev. B **64**, 245407 (2001).
[38]H. Singh and B. Dayal, J. Less Common Met. **18**(2), 172 (1969).
[39]K. Kamali, T. R. Ravindran, C. Ravi, Y. Sorb, N. Subramanian, and A. K. Arora, Phys. Rev. B **86**, 144301 (2012).
[40]M. Millot, R. T. Zaera, V. M. Sanjose, B. J. Marc, and J. Gonzalez, Appl. Phys. Lett. **96**, 152103 (2010).
[41]P. Verma, S. C. Abbi, and K. P. Jain, Phys. Rev. B **51**, 16660 (1995).